Int. J. Electrochem. Sci., 16 **(2021)** Article Number: 211010, doi: 10.20964/2021.10.33

International Journal of
ELECTROCHEMICAL
SCIENCE
www.electrochemsci.org

Effect of Magnetic Field on Corrosion Behavior of X52 Pipeline Steel in Simulated Soil Solution

Yong Yang, Yanlong Luo, Ming Sun, Junqiang Wang[*]

China Special Equipment Inspection and Research Institute, Beijing 100029
[*]E-mail: 39530354@qq.com

Received: 31 May 2021 / *Accepted:* 19 July 2021 / *Published:* 10 September 2021

Magnetic flux leakage detection is the primary method used for detecting metal damage in oil and gas pipelines. After a magnetic flux leakage test is used, a residual magnetic field remains in the steel pipeline for a long time. The influence that the residual magnetic field has on the corrosion behavior of the pipeline is not completely clear. The influence that the magnetic field has on the corrosion behavior of X52 pipeline steel in a simulated Yingtan soil solution was investigated using an open circuit potential, potentiodynamic polarization, electrochemical impedance spectroscopy, and corrosion morphology observation techniques. The results indicate that the magnetic field positively shifted the corrosion potential, increased the corrosion current density, reduced the charge transfer resistance, and basically had not impact on the corrosion morphology. When the magnetic field strength was stronger, the influence on the electrochemical corrosion behavior was greater. The influence that the magnetic field has on the electrochemical reaction process is comprehensively determined by multiple factors, such as the magnetic flux density near the electrode surface, the magnetic field gradient, the ion magnetism, and the concentration in the test electrolyte. These factors mainly promote or inhibit the corrosion process through the action of the Loren magnetic force and Kelvin force on the movement of the reactants and reaction products, such as Fe^{2+}, H^{+}, and O_2 in the solution. In this study, the magnetic field promoted the development of electrochemical corrosion as a whole.

Keywords: magnetic field, magnetic flux density, simulated Yingtan soil solution, corrosion behavior

1. INTRODUCTION

As of 2019, the length of China's oil and gas pipelines has reached 13.5×10^4 km[1]. Internal magnetic flux leakage detection is the primary method that is used for detecting metal damage in oil and gas pipelines[2]. During magnetic flux leakage testing, a steel pipeline is fully magnetized with a magnetic field magnitude of 1.4~1.8 Tesla. A residual magnetic field on the order of 0.3-1.5 T then remains in the steel pipeline for a period of several hours to several weeks after the magnetic flux leakage testing is complete [3]. Practical experience has shown that a pipeline can still exhibit residual

magnetism even two years after an internal magnetic flux leakage test. Whether the residual magnetic field has a significant impact on pipeline corrosion has become a concern of the pipeline transportation industry.

There is not yet consensus about the research conclusions regarding the effects of a magnetic field on metal corrosion. Most studies [4-7] have shown that steel in solution generates a magnetic overpotential when it is affected by a magnetic field, and this causes the electrode potential to shift positively. Yu [8] found that the corrosion potential of aluminum-magnesium alloys in NaCl solution was negatively shifted when the alloys were affected by a magnetic field. Some studies found that the magnetic field has an important influence on corrosion distribution. A magnetic field changes the state of the cathode and anode in natural corrosion [9]. The relative direction of the magnetic field and the metal corrosion surface [10, 11] obviously affect the distribution of a corrosion area. The effects that a magnetic field has on the corrosion rate of metals are also inconsistent. Ghabashy [12] found that the corrosion rate of steel in a ferric chloride solution was affected by an external magnetic field. When the external magnetic field was small, the corrosion rate caused by the magnetic field was lower than the natural corrosion rate, and when the external magnetic field was large, the corrosion rate was higher than the natural corrosion rate. Zhang [14] found that the corrosion rate of X80 steel in Shenyang meadow soil increased with an increase in the applied magnetic field. Hui [14] found that the magnetic field accelerated the corrosion rate of X60 steel in the soil of the Changsha area. Jackson[3] reported that the magnetic field aggravated defects in steel, such as pitting and cracks on the surface of the test sample. Espina-Hernández [15] found that the magnetic field inhibited the development of pitting corrosion. Wei [16] showed that the magnetic field can inhibit the microbial corrosion on Cu. Regarding the mechanism for the effect that a magnetic field has on corrosion behavior, it is generally believed that the magnetic field has little effect on the activation reaction process of the corrosion electrode [17, 18], whereas it has an important effect on the mass transfer of reactants and reaction products [18-20]. However, Sueptitz [21] found that when Fe corrosion in dilute sulfuric acid was affected by a magnetic field, the magnetic field that was perpendicular to the working surface of the electrode caused Fe^{2+} to move far away from the electrode and H^{+} to move close to the electrode; thus, the pH of the solution near the surface of the electrode decreased, and this resulted in an increase in the activation reaction current density. The Loren magnetic force and magnetic field gradient force are the main factors that affect mass transfer [20, 22, 23]. The relative direction of the magnetic field and the movement of the charged particles determine the direction of the Loren's magnetic force, and the magnetic field gradient and particle magnetism determine the direction of the magnetic field gradient force, which comprehensively affects the electrode reaction rate [24, 25]. However, in all of the above studies (except for the work by Espina-Hernández) the test samples and the solution were placed in an external uniform magnetic field that was significantly different from the residual magnetic field detected in the magnetic flux leakage.

Southeast China is a densely populated and economically developed region with a large number of oil and gas pipelines. The Yingtan red soil in the China southeastern region is a typical acidic soil with a high temperature, air proof, high water content, low oxygen content, a pH value in the range of 3-5, which is extremely corrosive to buried pipelines [26]. Open circuit potential (OCP) measurements, potentiodynamic polarization, electrochemical impedance spectroscopy (EIS), and corrosion morphology observation were used to study the influences that a magnetic field has on the corrosion

behavior of X52 pipeline steel in a simulated Yingtan soil solution. The mechanism for the influence that a magnetic field has on corrosion is also discussed. The research results provide a theoretical basis for the corrosion protection of X52 pipeline steel that is subjected to a magnetic flux leakage test .

2. EXPERIMENTAL

2.1 Materials and solutions

All of the samples that were investigated in this work were machined from an API X52 pipeline, which has the following chemical composition (wt %): C 0.20, Si 0.45, Mn 1.60, P 0.02, S 0.01, and Fe balance. As seen in Figure 1, the sample was a 10mm-wide ring cut from a Ø219×6mm tube, wound with 650 turns of insulated copper wire with a copper core diameter of 0.82mm. The part of the sample where the copper wire is not wrapped had an area of about Ø7mm and was used as the working surface. A simulated Yingtan soil solution was used as the test medium. In the electrochemical experiment, an electrolytic cell was processed with nylon plastic for the test. Also, a Ø7mm circular through-hole was processed on the bottom to connect the sample. The joint surface was sealed with a silicone gasket, and the working surface of the sample was immersed horizontally in the solution. Before the experiment, the working surfaces of the samples were sequentially wet ground with waterproof emery papers up to 600 grit and sequentially cleaned with alcohol and distilled water.

The test solution used for this study was a simulated Yingtan soil solution that contained [17] 0.222g/L $CaCl_2$, 0.936g/L NaCl, 0.284g/L Na_2SO4, 0.394 g/L $MgSO_4 \cdot 7H_2O$, 0.586g/L KNO_3, and 0.302g/L $NaHCO_3$. The chemicals were analytic grade reagents, and deionized water was used. NaOH and acetic acid solutions were added to adjust the pH of the solution to 4.1.

Figure 1. Sample used for tests

The potentiostat was a Gamry Reference 600+ Versastat device controlled by Framework V7.03 software. This setup was used to determine the OCP and potentiodynamic polarization curves and to carry out EIS measurements on an X52 steel electrode (working electrode). SCE served as the reference

electrode, and a platinum plate served as the counter electrode. The same potentiostat was used to measure the OCP values of samples with 4 different magnetic fields with a scan rate of 1mV/s. The first measurement time was 10 min, and the last measurement time was 20 min. Potentiodynamic polarization sweeps were recorded at a scan rate of 1 mV/s. EIS measurements were made under OCP conditions with a sinusoidal potential excitation of 10 mV amplitude over a frequency range of 0.01–10 kHz. OriginPro2017 was used to analyze the potentiodynamic test results, and ZSimpWin V3.60 was used to analyze the EIS results and to fit the data to equivalent circuits. Optical microscopes were used to observe the surface corrosion morphologies of the samples. The potential used in this study was relative to SCE.

DC currents of 0, 1A, 2A, and 3A were applied to the coils to induce different magnetic fields. The magnetic field was calculated using equation (1):

$$H = \frac{NI}{L} \quad (1)$$

where H is the magnetic field strength (A/m), N is the number of turns of the coil, I is the current value in the coil (A), and L is the length of the magnetic circuit (m). In this article, L is also the circumference of the ring sample.

The calculated magnetic flux density that generated by applying 1A, 2A, and 3A DC in the coil were 0.9, 1.9, and 2.8kA/m, respectively. Related research [27] showed that under a magnetic field of 4.5kA/m, the magnetic flux density of X52 steel is not greater than 1.5T; the samples in this study were all in different states of unsaturated magnetization.

3. RESULTS AND DISCUSSION

3.1 OCP

The time dependence of OCP for X52 pipeline steel in a simulated Yingtan soil solution that was subjected to different magnetic field strengths is shown in Figure 2. The corrosion potential of the sample positively shifted with an applied the magnetic field. The corrosion potential changed slowly under a magnetic field strength of 0.9kA/m. The corrosion potential fluctuated positively under a magnetic field strength of 1.9kA/m. Under a magnetic field strength of 2.8kA/m, the potential forward shifted quickly and then remained stable. In general, when the magnetic field strength was greater, the positive offset of the corrosion potential was greater. This result is consistent with the conclusions from related studies [4-7], which found that samples in a magnetic field generated a magnetically induced positive overpotential. The change in the corrosion potential indicates that when the magnetic field strength is greater, the thermodynamic stability of the sample under the magnetic field is worse.

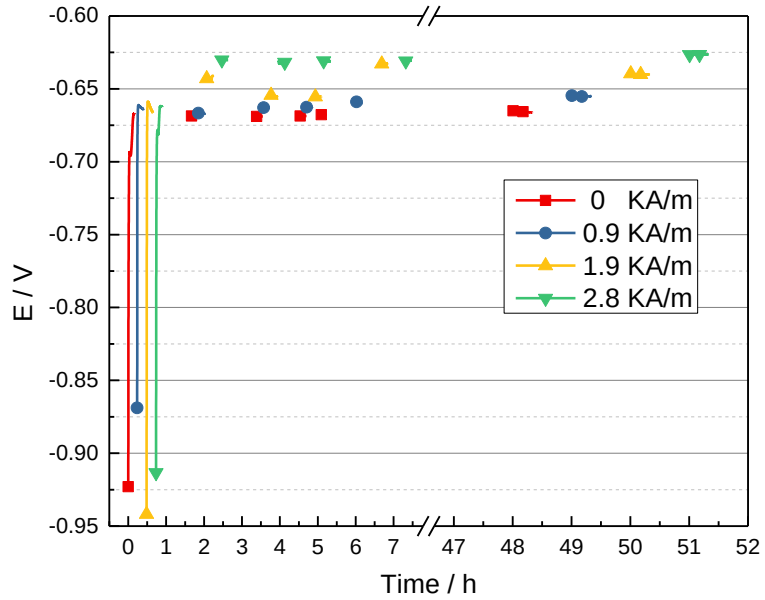

Figure 2. OCP vs immersion time of samples in a simulated Yingtan soil solution with magnetic field strengths

3.2 EIS

Figure 3 shows Nyquist plots for X52 pipeline steel that was immersed in simulated Yingtan solution for 1 h and for 48 h under magnetic fields. As seen from the figure, the electrochemical impedance spectroscopy under different magnetic field strengths exhibits a capacitive reactance arc, which indicates that the reaction process is controlled by electron transfer. As first judged by the size of the capacitive reactance arc radius, it was determined that when the magnetic field strength was greater, the electrochemical reaction impedance was smaller, and the corrosion resistance of the sample was weaker. EIS data were fitted with the equivalent circuit shown in Figure 4, and the fitting results are shown in Table 1. In the equivalent circuit, Rs represents the solution resistance, Q represents the constant phase angle element of the electric double layer capacitor, and Rt represents the charge transfer resistance. The charge transfer resistance of the sample that was under a magnetic field and immersed for 1 and 48 h was smaller than that of the sample that without a magnetic field. Also, it decreased with an increase in the magnetic field. Under a magnetic field of 1.9 and 2.8kA/m, Rt was slightly lower than Rt under natural corrosion conditions. However, under a magnetic field of 1.9 and 2.8kA/m, Rt was greatly reduced. At the beginning of immersion, the Rt values under the two magnetic field strengths are not much different, but as the immersion time was extended to 48 hours, the Rt value (126Ω•cm^2) under a magnetic field intensity of 2.8kA/m was clearly less than the Rt value under the magnetic field intensity of 1.9kA/m (165Ω•cm^2). Because of the influence of corrosion products, when the immersion time was increased, the Rt of the sample under the same magnetic field became larger. The dispersion index (n_{dl}) increased with an increase in the magnetic field; this indicates that when the magnetic field is larger, the corrosion current density distribution is more uniform. This should be because the magnetic field changes the distribution of the anode and cathode on the sample surface [9].

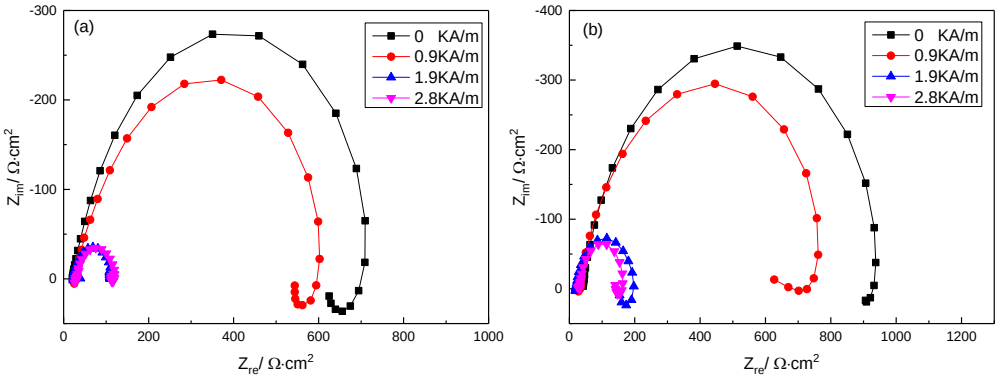

Figure 3. Nyquist plots of EIS of X52 pipeline steel samples immersed in simulated Yingtan soil solution for (a) 1h and (b) 48h with magnetic fields

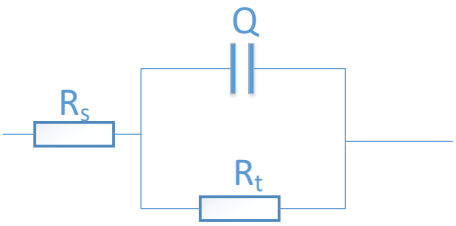

Figure 4. Equivalent circuit of EIS

Table 1. Equivalent circuit fitting for EIS data of samples in Yingtan soil solution

Immersionin g period (h)	Magnetic field (kA/m)	Rs (Ω•cm^2)	Ydl (Ssn/cm^2)	ndl	Rt (Ω•cm^2)
1	0	21	1.370×10^{-4}	0.8538	670
	0.9	27	1.224×10^{-4}	0.8565	557
	1.9	33	3.087×10^{-4}	0.8740	84
	2.8	20	4.176×10^{-4}	0.8825	86
48	0	35	2.196×10^{-4}	0.8333	913
	0.9	29	2.263×10^{-4}	0.8697	709
	1.9	22	1.365×10^{-3}	0.9299	165
	2.8	23	8.476×10^{-4}	0.9861	126

3.3 Potentiodynamic polarization

Figure 5 shows potentiodynamic polarization curves for X52 pipeline steel samples that were immersed in simulated Yingtan soil solution for 1h and 48h. The polarization curves show roughly similar characteristics; specifically, they show characteristics of typical active dissolution. Corrosion parameters obtained from the fitting of the polarization curves are shown in Table 2. Corrosion potential (Ec) increased with an increase in applied magnetic field strength, and this is consistent with results from OCP measurements. The Tafel slope (βa) of the anodic polarization curve was smaller than that (βc) of the cathodic polarization curve; this indicates that the corrosion control process was a cathodic reaction. Both βa and βc increased with an increase in magnetic field strength. Under a magnetic field of 0.9kA/m, the fitted corrosion current densities of the samples that were immersed for 1 h increased from 16.9

μA/cm^2 to 18.8 μA/cm^2 and that of the samples that were immersed for 48 h increased from 13.6μA/cm^2 to 20.6μA/cm^2. Under a magnetic field of 1.9 and 2.8kA/m, the corrosion current densities of the fitted samples were greatly increased compared to the case with no magnetic field. The corrosion current densities of the samples that were immersed for 1 h increased to 128.9 and 125.6 μA/cm^2, respectively, whereas the corrosion current density of the specimens that were immersed for 48 h increased to 75.1 and 96.6 μA/cm^2, respectively. That is, the applied magnetic field increased the corrosion rate of the sample. When the immersion time was prolonged, the natural corrosion rate decreased because of the inhibitory effect that corrosion products have on corrosion. In the case of a smaller magnetic field strength (0.9 kA/m), the corrosion rate increased with an increase in immersion time. When the size of the sample corrosion pit increased, the magnetic flux leakage increased, thereby enhancing the effect of the magnetic field. In the case of a smaller magnetic field strength (1.9 and 2.8 kA/m), the corrosion rate decreased with an increase in immersion time. Under a larger magnetic field, the magnetic flux leakage intensity that was generated by the smaller defects on the sample surface can affect the corrosion process, but the corrosion product inhibits the corrosion as time increases.

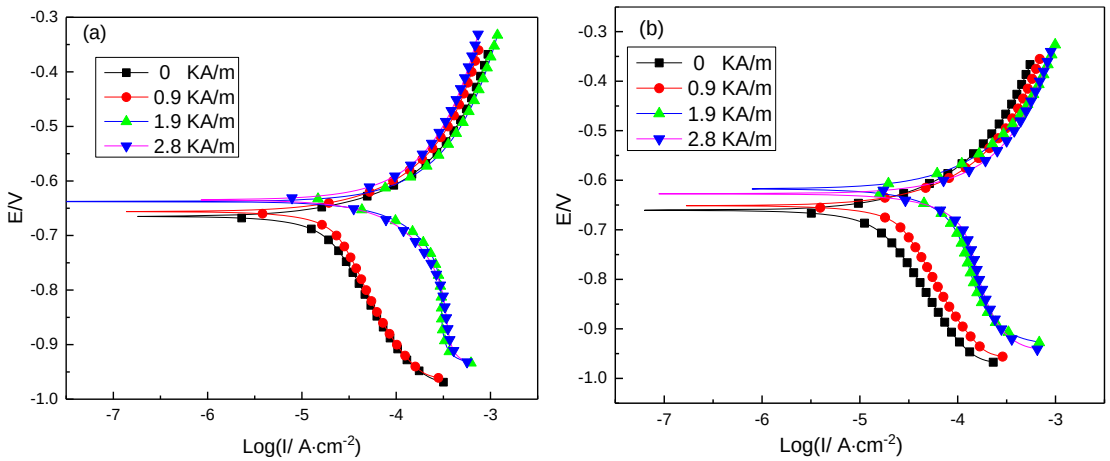

Figure 5. Potentiodynamic polarization curves of samples with magnetic fields immersed in a Yingtan soil solution for (a) 1h and (b) 48h

Table 2. Corrosion parameters of X52 steel with magnetic fields immersed in a Yingtan soil solution

Immersion period (h)	Magnetic field (kA/m)	Ec (mV)	βa (mV/dec)	βc (mV/dec)	Icorr (μA/cm^2)
1	0	-667	79	320	16.9
	0.9	-657	83	369	19.8
	1.9	-637	235	372	128.8
	2.8	-634	337	418	125.6
48	0	-660	93	309	13.6
	0.9	-652	99	353	20.6
	1.9	-625	180	680	75.1
	2.8	-613	201	743	96.6

3.4 Corrosion morphologies

Figure 6 shows corrosion morphology images of X52 pipeline steel that was immersed in a simulated Yingtan soil solution for 48 h under different magnetic field strengths. In the presence or absence of a magnetic field, the samples were uniformly corroded, and there was no obvious local corrosion. The natural corrosion process without a magnetic field was relatively light, and scratches on the surface of the sample are clearly visible. Corrosion in the presence of a magnetic field was obviously more serious, but the corrosion morphology under different magnetic field strengths was not significantly different.

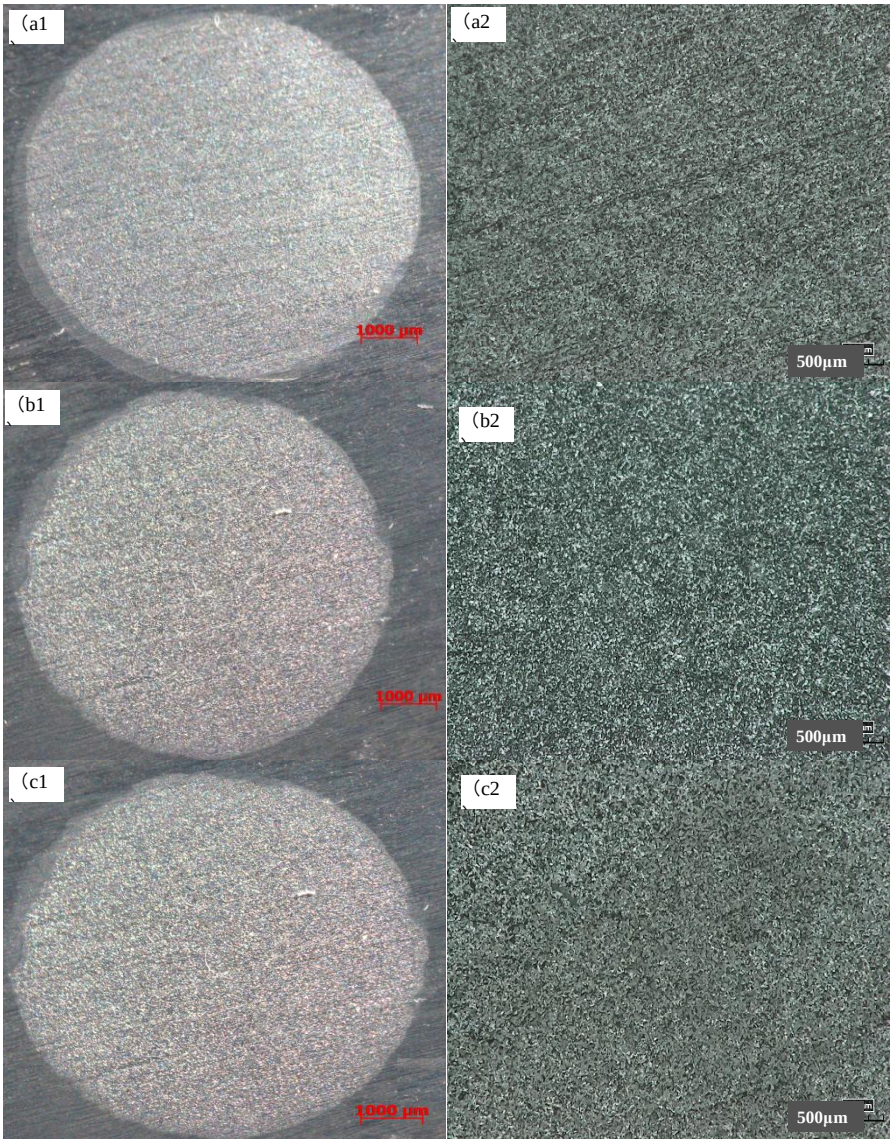

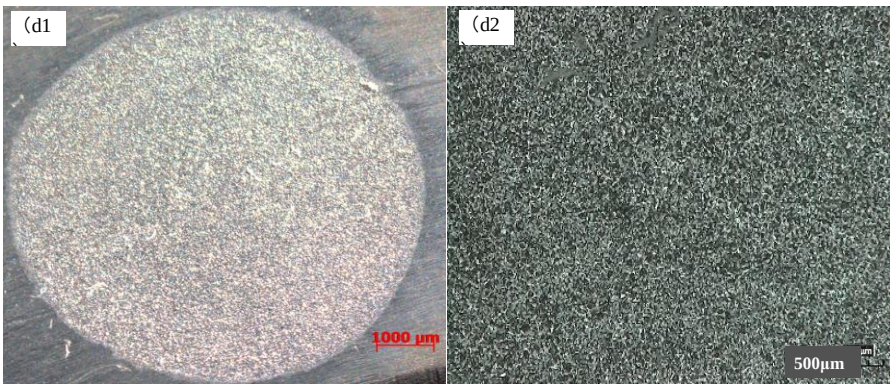

Figure 6. Optical photographs of X52 steel in a simulated Yingtan solution for 48h under 0 kA/m (a1,a2), 0.9 kA/m (b1,b2), 1.9 kA/m (c1,c2), and 2.8kA/m (d1,d2) magnetic fields

3.5 Mechanism analysis

In contrast to the situation where the applied magnetic field was perpendicular or parallel to the working surface of the electrode, the magnetic field that acted on the electrochemical reaction in this study resulted from a magnetic field that leaked from the surface of the sample after the sample was magnetized. The strength of the leaked magnetic field was determined by the surface roughness of the sample (equivalent to the surface minor defects). A schematic diagram of the leaked magnetic field that formed near small defects on the sample surface is shown in Figure 7. It is generally believed that the magnetic field has almost no effect on the electron transfer process of the electrode reaction [28] but that it has an obvious effect on the mass transfer process of the reaction [20, 21, 29]. The magnetic field mainly affects the mass transfer process through the Loren magnetic force [30], Kelvin force (magnetic gradient force) [31], and paramagnetic gradient force [20]. When charged ions move in a magnetic field, a Loren magnetic force (F_L) is produced, according to formula (2), where J is the energy density of the charged ions and B is the magnetic flux density.

$$F_L = J \times B \qquad (2)$$

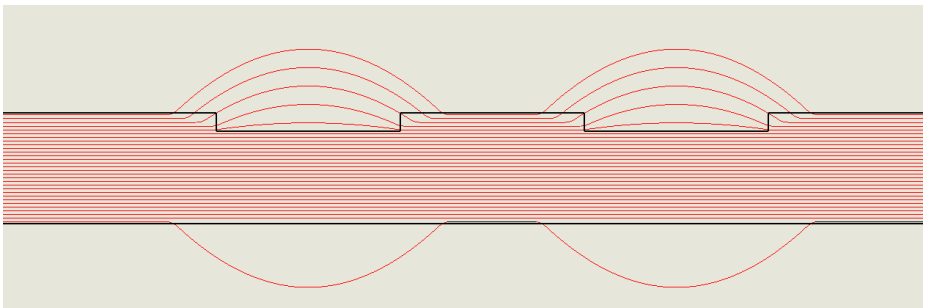

Figure 7. Schematic diagram of the distribution of the magnetic flux intensity on the surface of the sample

In the redox reaction, the ion concentration difference causes the ions to diffuse because of the continuous consumption of reactants and the continuous generation of reaction products. For example, Fe^{2+} is continuously generated on the electrode surface and diffuses into the solution, whereas H^+ diffuses to the electrode surface to participate in the reduction reaction. As seen in Figure 7, the diffusion of Fe^{2+} and H^+ crosses the lines of the magnetic force to generate F_L parallel to the electrode surface, thereby accelerating the diffusion of ions.

In a nonuniform magnetic field, there is a Kelvin force ($F_{B)}$ that causes paramagnetic particles to move to regions of higher magnetic flux density and diamagnetic particles to regions of lower magnetic flux density. The Kelvin force can be expressed as follows:

$$F_B = \frac{\chi_m cB\vec{\nabla}B}{\mu_0} \qquad (3)$$

where χ_m is the magnetic susceptibility per unit mass, c is the ion concentration, μ_0 is the absolute magnetic permeability, and $\vec{\nabla}B$ is the magnetic gradient.

The particle magnetism and concentration, magnetic flux density, and gradient value determine the value of F_B. The magnetic flux density distribution and ion magnetism determine the direction of ion movement. The magnetic flux density at the edge of the surface of the electrode and at geometric discontinuities is greater (as shown in Fig. 7). The Fe^{2+} and O_2 that are involved in the reaction in the test solution are paramagnetic [32], and H^+ is diamagnetic. Paramagnetic species tend to accumulate on the surface of the electrode and at the edges of geometric discontinuities; diamagnetic species tend to stay away from these locations.

Another important magnetic field force is the paramagnetic gradient force, which can be expressed as equation (4). This force is consistent with the ion concentration gradient direction, opposite to the ion diffusion driving force, and much smaller than the ion diffusion driving force [20]. Thus, the effect of this force on ion movement can be ignored.

$$F_P = \frac{\chi_m B^2\vec{\nabla}C}{2\mu_0} \qquad (4)$$

The main anode and cathode reactions in this study include:

$$Fe \rightarrow Fe^{2+} + 2e^- \qquad (5)$$

$$2H_2O + O_2 + 4e^- \rightarrow 4HO^- \qquad (6)$$

$$2H^+ + 2e^- \rightarrow H_2 \qquad (7)$$

The Loren magnetic force accelerates the movement of the microscopic solution, as a result of ion diffusion. Thereby, the thickness of the electric double layer [33] and the electrochemical reaction rate impedance are reduced (Figure 4). The migration effect that the Kelvin force has on different magnetic ions affects the corrosion process. When Fe^{2+} and O_2 accumulate in the region of higher magnetic induction, they inhibit the oxidation reaction and promote the reduction reaction to a certain extent. In this experiment, the reduction reaction is a control step, and therefore, it is more likely to promote corrosion development in general. In addition, the magnetic field also affects the hydration of the reactive ions, thereby changing the reactivity of the reactive ions. In summary, the promotion or inhibition of the electrochemical reaction by a magnetic field is determined by a combination of many

factors. These factors depend on the magnitude and gradient of the magnetic field on the electrode surface as well as the ion magnetism and concentration in the electrolyte. In this study, experiments showed that the magnetic field accelerates the corrosion; that is, the influencing factors caused by the magnetic field have a greater promotion effect than inhibition effect on corrosion.

4. CONCLUSIONS

(1) In a simulated Yingtan soil solution, a magnetic field causes the corrosion potential of X52 pipeline steel to shift negatively, corrosion current density to increase, reaction charge transfer resistance to decrease, and the corrosion morphology to change to a certain extent.

(2) In a simulated Yingtan soil solution, when the magnetic field is greater, the impact on the electrochemical corrosion behavior of X52 pipeline steel is greater.

(3) The influence that a magnetic field has on the electrochemical reaction process is comprehensively determined by multiple factors, such as the magnetic flux density, magnetic field gradient, and particle magnetism and concentration in the electrolyte. In a simulated Yingtan soil solution, the corrosion promotion effect that the magnetic field has on the X52 pipeline steel is greater than the corrosion inhibition effect, thus accelerating electrochemical corrosion as a whole.

ACKNOWLEDGEMENTS
This research was supported by the Science and Technology Plan Projects of State Administration for Market Regulation (2019MK136), CSEI Research Program (2019-Youth-03).

References

1. Z.W. Nie, J. Huang, Y.Z. Yu, Y.J. Wang, C. Shan, *Oil Gas Storage Transp*., 39(01)(2020)16.
2. L.J. Yang, H. Geng, S.W. Gao, *Chin. J. Sci. Instrum*.,37(08)(2016)1736.
3. J. E. Jackson A.N. Lasseigne-Jackson, F.J. sanchez, D.L. Olson, B. Mishra. The Influence of Magnetization on Corrosion in Pipeline Steels: 6th International Pipeline Conference, Alberta, Canada, 2006[C].
4. C. Wang, J.M. Chen. *J. Chin. Soc. Corros.Prot*., 14(02)(1994)123.
5. Z.P. Lu, J.M. Chen. *J. Chin. Soc. Corros.Prot*., 17(01)(1994)27.
6. Z.P. Lu, D.L. Huang, W. Yang. *Corros. Prot*., 23(05)(2002)185.
7. S.W. Cai, F. Ning, Y.J. Tang, K. Zhang, T.M. Cui. *Corros. Prot*., 41(08)(2020)1.
8. X. Yu, M.N. Zhu, X.J. Li, S.F. Wang, W.C. Zhuang. *Mod. Salt Chem. Ind.*, 46(03)(2019)8.
9. R.Z. Liu. *Plating & Finishing*, 12(06)(1985)8.
10. Z.P. Lu, T. Shoji, W. Yang. *Corros. Sci*., 52(2010)2680
11. Z.P. Lu, D.L. Huang, W. Yang, *J. Congleton. Corros. Sci*., 45(2003)2233.
12. M.A. Ghabashy. *Anti-corros. method*. M., 35(1988):12.
13. K.N. Zhang, M. Wu, F. Xie, D. Wang, Y.X. San. *J. Chin. Soc. Corros.Prot*., ,37(02)(2017)148.
14. H.J. Hui, Q.S. Dai, K.Chen, Z.T. Jiang, W.Cui, Y.F. Li. *Corros. Prot*., 40(07)(2019)474.
15. J.H. Espina-Hernández, F. Caleyo, V. Venegas, J.M. Hallen. *Corros. Sci*.,53(2011)3100.
16. X.Y. Wei, M. Moradi, L.J. Yang, Z.P. Lu, B.C. Zheng, Z.L. Song. *J. Chin. Soc. Corros.Prot*.,

39(06)(2019)484.
17. R. Sueptitz, K. Tschulik, M. Uhlemann, L. Schultz, A. Gebert. *Corros. Sci*., ,53(2011)3222.
18. Z.P. Lu, C.B. Huang, D.L. huang, Y. Wu. *Corros. Sci*., ,48(2006)3049.
19. O. Aaboubi, J.P Chopart. ,J. Douglade, A. Olivier. *J. Electrochem. Soc*., 137(1990)1796.
20. G. Hinds, J.M.D. Coey, M.E.G. Lyons. *Electrochem. Commun*., ,3(2001)215.
21. R. Sueptitz, K. Tschulik, M. Uhlemann, L. Schultz, A. Gebert. *Electrochim. Acta*, 56(2011)5866.
22. R. Sueptitz, J. Koza, M. Uhlemann, A. Gebert, L. Schultz. *Electrochim. Acta*, 54(2009):2229.
23. X.P. Wang, J.J. Zhao, Y.P. Hu, L. Li, C. Wang. *Electrochim. Acta*, 117(2014)113.
24. O.Lioubashevski, E. Katz, I. Willner. *J. Phys. Chem. C,* , 111(2007)6024.
25. X.J. Li, M. Zhang, B.Y. Yuan, L.Li, C.Wang. *Electrochim. Acta*, 222(2016)619.
26. Z.Y. Liu, G.L. Zhai, C.W. Du. *Acta Metal. Sin*. , 2(2008)209.
27. R. Grossinger, F. Keplinger, N. Mehmood, H. Espina-Hernadez. *IEEE Trans. Magn*., 44(2008)3277.
28. O. Devos, O. Aaboubi, J. Chopart, A. Olivier. *J. Phys. Chem*. A, 104(2000)1544.
29. K.M. Grant, J.W. Hemmert, H.S. White. *J. Am. Chem. Soc*., 124(2002)462.
30. L.M.A. Monzon, J.M.D. Coey. *Electrochem. Commun*., 42(2014)38.
31. L.M.A. Monzon, J.M.D. Coey. *Electrochem. Commun*., 42(2014)42.
32. D.R. Lide. Magnetic susceptibility of the elements and inorganic compounds, in: D.R. Lide (Editor in Chief), Handbook of Chemistry and Physics, CRC Press, 2004, pp. 4–143.
33. G. Kamesui, K. Nishikawa, H. Matsushima, M. Ueda, *J. Electrochem. Soc*., 168(2021)31507.